

Shape Deformation and Circle Instability in Two-Dimensional Lipid Domains by Dipolar Force: A Shape- and Size-Dependent Line Tension Model

Mitsumasa Iwamoto¹ and Ou-Yang Zhong-can²

¹*Department of Physical Electronics, Tokyo Institute of Technology, 2-12-1 O-okayama, Meguro-ku, Tokyo 152-8552, Japan*

²*Institute of Theoretical Physics, The Chinese Academy of Sciences, P.O.Box 2735 Beijing 100080, China*

(Received 3 April 2003; revised manuscript received 30 August 2004; published 10 November 2004)

The dipolar energy of a solid monolayer domain surrounded by a fluid phase at an air-water interface is derived approximately as a sum of an additionally negative line tension and a curvature-elastic energy at the boundary. Variation of the domain energy yields an equilibrium domain shape equation. The obvious solutions of the domain shape equation clearly predict a circle, torus, *D*-form, *S*-form, and serpentine manner shape found experimentally, depending on the difference in the Gibbs free energy between the solid and fluid phases and the total line tension. Analysis of linear instability for a circle with a fixed area shows that, above a threshold size, the circle can be deformed into an *m*-sided quasipolygon. The good agreement with the observation and numerical calculation reported by Lee and McConnell [J. Phys. Chem. **91**, 9532 (1993)] shows the quantitative validity of the present theory.

DOI: 10.1103/PhysRevLett.93.206101

PACS numbers: 68.03.-g, 02.40.Hw, 68.15.+e, 68.70.+w

Monolayers of lipid on the water surface have been studied for more than a century, and the aspect of different phases and their coexistence in these two-dimensional (2D) systems has been expected in analogy with 3D ones [1]. Such predictions have been directly visualized by using fluorescence microscopy, etc. [2,3]. The microscopic observation revealed a variety of ordered and disordered domain shapes and behaviors of monolayers [4]. Among them, circular shapes of solid domain surrounded by fluid phase, and deformed shapes of their transitions to torus [5], *D* form, *S* form, serpentine manner form [6,7], and *m*-sided quasipolygon form [8,9] are of interest, and these 2D shapes have attracted a number of studies [9–13]. In analogy with smectic-*A* liquid crystal bilayer, Helfrich proposed that the shape energy of a 3D vesicle be given by

$$F = \Delta P \int dV + \lambda \oint dA + \frac{k_c}{2} \oint (2H + c_0)^2 dA, \quad (1)$$

where ΔP is the osmotic pressure; λ is the tensile stress acting on the membrane; A and V are the surface and volume elements, respectively; k_c is the bending rigidity, H the mean curvature, and c_0 the spontaneous curvature. The last term represents the curvature-elastic energy F_c . Calculating the first variation of F with consideration of ΔP and λ as Lagrange multipliers, the 3D equilibrium-shape equation was derived as [14]

$$\Delta P - 2\lambda H + 4k_c \left(H + \frac{1}{2} c_0 \right) \times \left(H^2 - K - \frac{1}{2} c_0 H \right) + 2k_c \nabla^2 H = 0, \quad (2)$$

where K is Gaussian curvature, and ∇^2 is the Laplace-Beltrami operator. Using (2), the 3D curve cases such as the coil formation of carbon nanotubes [15], growth of smectic-*A* filaments [16], and others have been solved reasonably. On the other hand, the pioneering work con-

cerning the shape energy of 2D domains was done by the McConnell group. The shapes of domains in equilibrium and their deformation were understood in terms of a competition between line tension and long range electrostatic force induced by molecular dipoles in domains, i.e., minima of the domain energy [12]. Comparing with the model by McConnell [13], in analogy with the Helfrich curvature-elastic energy of (1), we introduce additionally a Lagrange multiplier ΔP , taking into account the constraint of constant domain area and/or the difference in the Gibbs free energy density between outer (e.g., fluid) and inner (solid) phases, i.e., $\Delta P = -g_0$. Then the shape energy of a 2D domain is expressed as

$$F = \Delta P \int dA + \gamma \oint ds - \frac{\mu^2}{2} \oint \oint \frac{\vec{t}(l) \cdot \vec{t}(s)}{|\vec{r}(l) - \vec{r}(s)|} dl ds, \quad (3)$$

where γ is the line tension; μ is the dipole density; $\vec{r}(s)$ describes the domain boundary curve; s is the arclength; and $\vec{t} = d\vec{r}/ds$, the unit tangential vector of the boundary. Here $g_0 > 0$, since solid phase is more stable than fluid one. This viewpoint has been used to consider the smectic-*A* phase grown from isotropic phase [17]. (3) is similar to (1). Instead of the curvature-elastic energy F_c [the last term of (1)], the origin is the electrostatic dipole-dipole interaction energy [the last term of (3)]. In this model, all dipoles align in the same direction normal to the water surface, in a manner similar to the director alignment in the smectic-*A* liquid crystal bilayer. The first two terms favor circular shape domains according to the 2D Young and Laplace law (1805), whereas the last term favors other phases with longer perimeter and different shapes such as thin slab [18]. In the earlier studies, the researchers assumed *a priori* the existence of equilibrium domains with some regular shapes, e.g., circle [10,12] and torus [11], and calculated their domain energy with (3). Then they calculated their equilibrium domain size by

variation of the energy with respect to size parameter. However, the experimental findings of noncircular shapes, such as D and S forms, and serpentine ones, have not been successfully analyzed. The long-lasting insufficient stage of the 2D domain theory is due to the mathematical difficulty in calculating the doubleline integral, the last term of (3). In this Letter, we try to provide an approach to overcome this mathematical difficulty. The doubleline integral of the dipolar energy has been approximately derived as a sum of an additionally negative line tension and a curvature-elastic energy of the domain boundary. This derived expression enables us to calculate the δF analytically. As a result, D and S forms, and serpentine manner forms are shown to be its solutions, depending on ΔP , total line tension, and the dipole force-induced curvature-elastic modulus. The infinitesimal instability of a circle with fixed area can also be analyzed, and it is found that below some negative threshold line tension, the circle can be deformed into a shape associated with m th order harmonics. The comparison of the obtained formula with the observation and numerical examples calculated directly from the doubleline integral previously by Lee and McConnell [9] shows the validity of the present theory.

The key step is to rewrite the dipolar force energy as

$$F_\mu = -\frac{\mu^2}{2} \oint \left(\oint \frac{\vec{t}(s) \cdot \vec{t}(s+x)}{|\vec{r}(s+x) - \vec{r}(s)|} dx \right) ds, \quad (4)$$

where arc variable x is defined as $x = l - s$. With $\vec{t} = d\vec{r}/ds = \vec{r}_s$ and Frenet formulas of a plane curve [19]: $d\vec{t}/ds = \kappa(s)\vec{m}$, $d\vec{m}/ds = -\kappa(s)\vec{t}$, where $\kappa(s)$ and $\vec{m}(s)$ are the curvature and unit normal vector of the boundary curve at s , and $\vec{t}(s+x)$ and $\vec{r}(s+x)$ are expected as

$$\vec{t}(s+x) = \vec{t}(s) + \kappa(s)\vec{m}(s)x + \frac{1}{2}[\kappa_s\vec{m}(s) - \kappa^2(s)\vec{t}(s)]x^2 \dots, \quad (5)$$

$$\vec{r}(s+x) = \vec{r}(s) + \vec{t}(s)x + \frac{1}{2}\kappa(s)\vec{m}(s)x^2 \dots. \quad (6)$$

Substituting (5) and (6) into (4) gives the expression of the dipole force energy in a generalized line tension energy form as $F_\mu = \oint \bar{\lambda}(\kappa, \kappa_s, \dots) ds$, where $\bar{\lambda}$ is a series of $\kappa(s)$ and its derivatives. If we consider a somewhat smooth curve, only take into account the first two terms of F_μ series as Taylor approximation and using the monolayer thickness h , nonzero, as the cutoff, we can approximately obtain the expression given by

$$F_\mu \approx -\frac{\mu^2}{2} \oint \ln \frac{L}{h} ds + \frac{11\mu^2}{96} L^2 \oint \kappa^2(s) ds, \quad (7)$$

where L is the boundary length. The role of h as a cutoff has been illustrated in [18] and agreed by Lee and McConnell by assuming *ansatz* of $h = e^{1/2}\Delta$ [Eq. (46) in [9] where Δ is the dipole-dipole separation distance,

the cutoff in their calculation] [9]. So far, we have not provided a clear answer to the physical basis for our Taylor expansion of the dipolar interaction; however, we can show it is efficient in mathematics when the ratio of the distance between two adjacent dipoles to the radius of domain boundary is small. Actually, as observed in experiment, the radius of domain is on the order of micrometers and quite larger than the distance of adjacent dipoles. Thus, it is always satisfied that the parameter in expansion is small. For an exact calculation for a circle of radius ρ_0 , the logarithmic divergence is calculated as $\ln(8\rho_0/e^{1/2}h) \approx \ln(5\rho_0/h)$ (see (2.11) in Ref. [18]), and this is nearly equal to $\ln \frac{2\pi\rho_0}{h}$ as our present result with Taylor expansion approach. In fact, such an *ansatz* approach by expanding the line integral was also proposed by Langer, *et al.*, (see, (4.11) and (4.12) in ref. [18]) without further justification. Although the McConnell group has provided sound theoretical calculation to explain the domain shape bifurcation diagram for somewhat regular shapes [10,12], the expression (7) has extended the study to general shapes. From (7), one can find that 2D line tension is size- and shape-dependent. Thus the domain energy has the form

$$F = \Delta P \int dA + \lambda \oint ds + \alpha \oint \kappa^2 ds, \quad (8)$$

where $\lambda = \gamma - \frac{\mu^2}{2} \ln \frac{L}{h}$ is total line tension which is positive or negative dependent on γ , L , μ , and h . $\alpha = \frac{11}{96} \mu^2 L^2$ is certainly positive, and is regarded as the modulus of line curvature elasticity or 1D bending rigidity.

To obtain the equilibrium-shape equation, we have to derive variation equation $\delta F = 0$. It can be derived directly with 2D curve variation; however, in what follows we would like to map it onto the well known Helfrich model of a 3D fluctuation membrane vesicle. Thus, one can find the physics behind the above Taylor expansion such as the physics meanings of the parameters α , γ , and so on. Moreover, one can understand the strange shapes of present 2D domains by mapping it onto the well understood fluctuation of 3D cylinder vesicle. For 3D curve cases, we encountered this problem and completed the variation (2). For 2D curve cases, fortunately, there is no need to do it afresh due to the similarity of the expression of (1) and (8). Starting from the 3D equilibrium-shape equation of membrane vesicle with Helfrich model [20] (Eq. (2) in [14]), we can obtain the 2D curve solution of $\delta F = 0$ given by (8). In mathematics, by letting $2H = \kappa$, $c_0 = 0$, $K = 0$, $k_c \rightarrow 2\alpha$, and $\nabla^2 \rightarrow d^2/ds^2$, we can change the shape equation of the 3D vesicle into that for a 2D domain [21]

$$\Delta P - \lambda\kappa + \alpha\kappa^3 + 2\alpha\kappa_{ss} = 0, \quad (9)$$

where $\lambda = \gamma - \frac{\mu^2}{2} \ln \frac{L}{eh} + \frac{11}{48} L \mu^2 \oint \kappa^2 ds$ is slightly different from the definition in (8) due to the variation to L . The

normal expression shows clearly that λ depends not only on the boundary length but also on its shape.

Here one must note that ΔP and λ in (2) are the 3D pressure and surface tension, respectively, while in (9), they are 2D pressure and line tension, and so for k_c and α . Furthermore, both equations are derived by defining the normal direction as outward vesicle and solid domain, respectively. Therefore we have $H = -1/R_0$ for a sphere of radius R_0 , and $\kappa = -1/\rho_0$ for a circle of radius ρ_0 . According to this definition, $\kappa = 1/\rho_i$ then describes the curvature of inner circle of a torus with inner circle of radius ρ_i . Given these, it is understandable that outer and inner circles can coexist. In the case of planar curves, by rewriting (9) as a function $\Delta P(\kappa) = \lambda\kappa - \alpha\kappa^3$ and considering $\alpha > 0$, we illustrate the behavior of ΔP in Figs. 1(a) and 1(b) for $\lambda > 0$ and $\lambda \leq 0$, respectively. From Fig. 1, solutions can be theoretically divided into three cases: (i) Two circles and two *tori* of different sizes can coexist for $\lambda > 0$ and $0 > \Delta P > -\frac{2\sqrt{3}}{9} \frac{\lambda\sqrt{\lambda}}{\sqrt{\alpha}}$; (ii) Only one circle can exist for $\Delta P > 0$; and (iii) No compact circular domains can exist for $\lambda < 0$ and $\Delta P < 0$.

Case (ii) can easily be understood in mechanics: A negative tension and the elastic force ($\alpha > 0$) favor increasing the circle size, whereas a positive ΔP favors decreasing it; therefore, there exists an equilibrium size at which two tendencies balance. In case (iii) three forces are all outward; hence, they cannot balance each other. With such ideas, case (i) describes the solid domains grown in liquid phase and is then understandable; e.g., at inner circle of the equilibrium torus, both tension and elastic forces point to solid phase. On the other hand, the pressure points to a fluid phase because $\Delta P < 0$ (in physics, $\Delta p = -g_0$, this is like the ice formation at temperature of 0°C). In the previous experiments, we have found evidence for the above prediction. Two torus-shaped domains of *different sizes* are shown in Fig. 10 in [5]. Predicted two circles of different sizes are found in Fig. 4 in [7]. The coexistence of two *tori* and two circles have not been predicted by the McConnell group. They showed only one equilibrium circle with radius of $\frac{e^3 \Delta}{8} e^{\lambda/\mu^2}$. The usefulness of the present approach is also in the understanding on other noncircular domains which can be approximately and straightly explained by the above analysis. In case (i), Fig. 1(a) shows that the inner circle has more small radius than those of outer circles. The so-called *D* form shown in Fig. 1 and Fig. 5(d) in [7] can be seen as combinations with arcs of the three circles of radius ρ_i , ρ_{01} , and ρ_{02} , respectively. The *S*-like domain shown in Fig. 3 in Ref. [6], in principle, can be seen as the formation of *D* form but with $\Delta P \rightarrow 0$. In the same Figure, a torus appears which is obvious by closing the *D* form, i.e., created by circles of radius ρ_{02} and ρ_i . The formation of serpentine-like-tripe domains (see Fig. 5(c) in [7]) is the same as that of *S*-like domain but with ΔP more near to zero [Fig. 1(a)]. In fact, the general solutions

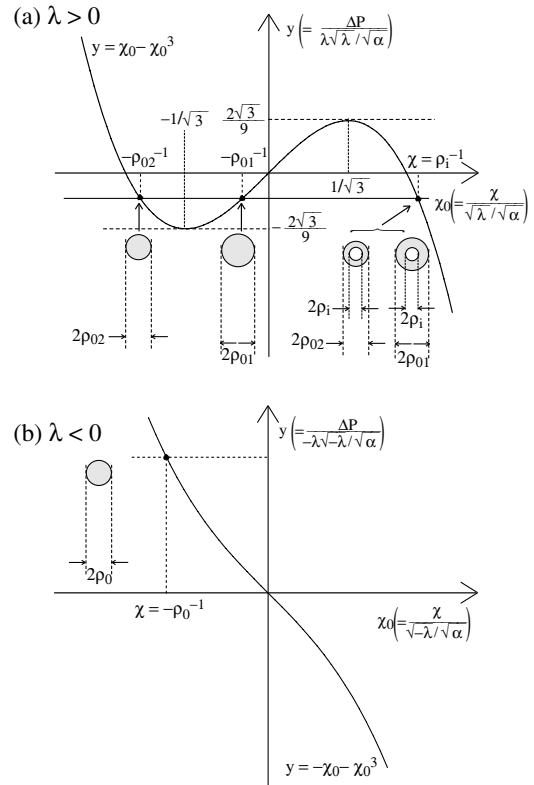


FIG. 1. Illustration of the equilibrium-circle shape equation of $\Delta P = \lambda\kappa - \alpha\kappa^3$, (a) for $\lambda > 0$ and (b) for $\lambda < 0$. In practical calculation, we use dimensionless equations $\Delta P_0 = \kappa_0 - \kappa_0^3$ and $\Delta P_0 = -\kappa_0 - \kappa_0^3$, i.e., (a) $\Delta P_0 = \Delta P/(\lambda\sqrt{\lambda}/\sqrt{\alpha})$ and $\kappa_0 = \kappa/(\sqrt{\lambda}/\sqrt{\alpha})$ and (b) $\Delta P_0 = (-\lambda\sqrt{-\lambda}/\sqrt{\alpha})$ and $\kappa_0 = \kappa/(\sqrt{-\lambda}/\sqrt{\alpha})$.

of (9) at $\Delta P = 0$ has been solved, in dealing with cylindrical vesicle shape problem [21]. Among them, a periodic shape shown in Fig. 1, Ref. [21] is just the case of the serpentine tripe. In the 3D case, (9) at $\Delta P = 0$ gives the helical coil for carbon nanotube [15] and the present serpentine stripes can refer to 2D helices. All these show the advantage of mapping the McConnell 2D domain shape problem to the Helfrich 3D vesicle shape problem. We shall give a more detailed example. The quasipolygon domain can be seen as a branching phenomenon of the instability of a circle of radius ρ_0 . We consider a slightly distorted circle $\rho = \rho_0 + \sum_m b_m \exp(im\phi)$, where $i \cdot i = -1$, $0 \leq \phi \leq 2\pi$, $m = 0, \pm 1, \dots, \pm\infty$, and $b_m^* = b_{-m}$. The variations of domain area, boundary length, and the curvature-elastic energy can be directly obtained by using the variation result of a cylindrical vesicle of radius ρ_0 , the formulas given by (69-71) in Ref. [22], respectively. Thus we have

$$\delta \oint ds = \pi\rho_0 \left[2(b_0/\rho_0) + \sum_{m=0}^{\infty} m^2 \left| \frac{b_m}{\rho_0} \right|^2 \right], \quad (10)$$

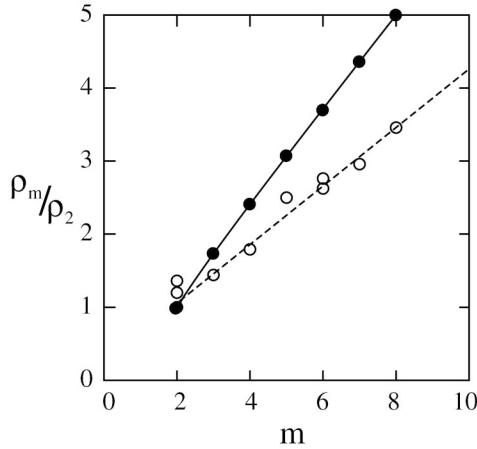


FIG. 2. Diagram illustrating how the sizes of experimentally observed domains with m -fold distortions correspond to theoretically calculated ones for harmonic shape transition. Dashed line shows the *ab initio* calculated results and circle points are experimental measurements, both of which follow Fig. 7 in [9]. The solid line and full circles are obtained from the present prediction, $\rho_m/\rho_2 = \sqrt{2m^2 - 3}/\sqrt{5}$.

$$\delta \int dA = \pi \rho_0^2 \left[2(b_0/\rho_0) + \sum_{m=0}^{\infty} \left| \frac{b_m}{\rho_0} \right|^2 \right], \quad (11)$$

$$\delta \oint \kappa^2 ds = \pi \rho_0^{-1} \left[-2(b_0/\rho_0) + \sum_{m=0}^{\infty} (2m^4 - 5m^2 + 2) \right. \\ \left. \times \left| \frac{b_m}{\rho_0} \right|^2 \right]. \quad (12)$$

To compare with previous calculations [9], we consider the case of $\delta A = 0$ and $\lambda < 0$, i.e., to maintain domain area constant; thus we obtain the linear term $(b_0/\rho_0) = -\frac{1}{2} \sum_m |b_m/\rho_0|^2$. Substituting into (8), (10), and (12) yields the deformation energy

$$\delta F = \pi \sum_{m=0}^{\infty} [\lambda \rho_0 + \alpha \rho_0^{-1} (2m^2 - 3)] (m^2 - 1) \left| \frac{b_m}{\rho_0} \right|^2. \quad (13)$$

The trivial case of $m = 1$, characterized by $\delta F = 0$, means a translation of the circle. The m th harmonic deformation can happen when the coefficient of $|b_m/\rho_0|$ in (13) becomes negative; i.e., the domain increases to the condition of $\rho_0 > \rho_m$ with $\rho_m = \sqrt{(2m^2 - 3)(\alpha / -\lambda)}$, ($m \geq 2$).

Thus we have the simple and analytic expression of $\rho_m/\rho_2 = \sqrt{2m^2 - 3}/\sqrt{5}$ that has been numerically shown in Fig. 2. In Fig. 2, the *ab initio* calculation results directly from (3) and (4) and the experimental measurements (Fig. 7 in [9]) performed by McConnell's group are also given. The comparison of our calculation with the *ab initio* ones and experiments does show good agreement. This again gives evidence of the present approach.

In summary, our discussion shows that the previous observation and *ab initio* calculation of circle instability do confirm the present model of great simplification by reducing the dipolar interaction, the doubleline integral, as a curvature-elastic energy plus a constant negative line tension. The obtained result is not only important in the simplifying calculation but also has its fundamental significance. It reveals that the line tension of a solid 2D-domain is both shape- and size-dependent [(7) and (9)].

-
- [1] A. Pockels, *Nature (London)* **43**, 437 (1891); I. Langmuir, *J. Am. Chem. Soc.* **39**, 1848 (1917); N. K. Adam, *The Physics and Chemistry of Surfaces* (Oxford University Press, London, 1941).
 - [2] M. Lösche *et al.*, *Ber. Bunsen-Ges. Phys. Chem.* **87**, 848 (1983).
 - [3] H. M. McConnell *et al.*, *Proc. Natl. Acad. Sci. U.S.A.* **81**, 3249 (1984).
 - [4] C. Knobler, in *Advances in Chemical Physics*, edited by I. Prigogine and S. A. Rice (Wiley, New York, 1990), Vol. 77, p. 397.
 - [5] R. M. Weis *et al.*, *J. Phys. Chem.* **89**, 4453 (1985).
 - [6] H. E. Gaub *et al.*, *J. Phys. Chem.* **90**, 1721 (1986).
 - [7] K. J. Stine and D. T. Stratmann, *Langmuir* **8**, 2509 (1992).
 - [8] R. M. Weis *et al.*, *Nature (London)* **310**, 47 (1984).
 - [9] K. Y. C. Lee *et al.*, *J. Phys. Chem.* **97**, 9532 (1993).
 - [10] D. Andelman *et al.*, *Acad. Sci., C* **301**, 675 (1985); D. Andelmann *et al.*, *J. Chem. Phys.* **86**, 3673 (1987).
 - [11] D. Keller, J. P. Korb *et al.*, *J. Phys. Chem.* **91**, 6417 (1987).
 - [12] H. M. McConnell *et al.*, *J. Phys. Chem.* **92**, 4520 (1988).
 - [13] H. M. McConnell, *J. Phys. Chem.* **94**, 4728 (1990).
 - [14] Z.-c. Ou-Yang *et al.*, *Phys. Rev. Lett.* **59**, 2486 (1987).
 - [15] Z.-c. Ou-Yang *et al.*, *Phys. Rev. Lett.* **78**, 4055 (1997).
 - [16] H. Naito *et al.*, *Phys. Rev. E* **55**, 1655 (1997).
 - [17] H. Naito *et al.*, *Phys. Rev. Lett.* **70**, 2912 (1993).
 - [18] S. A. Langer *et al.*, *Phys. Rev. A* **46**, 4894 (1992).
 - [19] M. P. do Carmo, *Differential Geometry of Curves and Surfaces* (Prentice-Hall, NJ, 1976).
 - [20] W. Helfrich, *Z. Naturforsch.* **28C**, 693 (1973).
 - [21] S. G. Zhang *et al.*, *Phys. Rev. E* **53**, 4206 (1996).
 - [22] Z.-c. Ou-Yang *et al.*, *Phys. Rev. A* **39**, 5280 (1989).